

Selective Human Adenosine A₃ Antagonists based on Pyrido[2,1-*f*]purine-2,4-diones: Novel Features of hA₃ Antagonist Binding

Eva-María Priego,^[b] María-Jesús Pérez-Pérez,^[b] Jacobien K. von Frijtag Drabbe Kuenzel,^[c] Henk de Vries,^[c] Adriaan P. IJzerman,^[c] María-José Camarasa,^[b] and Sonsoles Martín-Santamaría*^[a]

We should like to dedicate this paper to the memory of Jacobien von Frijtag Drabbe Kuenzel

Based on our previous results on the potent antagonist effect of 1*H*,3*H*-pyrido[2,1-*f*]purine-2,4-diones at the human A₃ adenosine receptor, new series of this family of compounds have been synthesized and evaluated in radioligand binding studies against the human A₁, A_{2A}, A_{2B} and A₃ receptors. A remarkable improvement in potency, and most noticeable, in selectivity has been achieved, as exemplified by the 3-cyclopropylmethyl-8-methoxy-1-(4-methylbenzyl)-1*H*,3*H*-pyrido[2,1-*f*]purine-2,4-dione (**10**) that combines a very high affinity at hA₃ (K_i = 2.24 nM), with lack of affinity for

the A₁, A_{2A} and A_{2B} receptors. On the basis of the published hA₃ receptor model (PDB 1OEA), molecular modeling studies, including molecular dynamics (MD) simulations, have been performed to depict the binding mode of the 1*H*,3*H*-pyrido[2,1-*f*]purine-2,4-diones and to justify the selectivity against the other adenosine receptors. These studies have led to novel features of the cavity where our antagonists are bound so that the cavity is lined by the hydrogen-bonded Gln 167-Asn 250 pair and by the highly conserved Phe 168.

Introduction

The neuromodulator adenosine acts by stimulating four cell surface receptors classified as subtypes A₁, A_{2A}, A_{2B} and A₃, all members of the superfamily of G-protein-coupled receptors.^[1] The four adenosine receptors have been pharmacologically characterized and cloned, the most recently being the A₃ subtype in the early 1990s.^[2] Activation of the A₃ adenosine receptor has been shown to mediate adenylate cyclase inhibition,^[2] stimulation of phospholipase C^[3] and D,^[4] and the release of inflammatory and allergic mediators from mast cells.^[5] Potential

therapeutic applications of this receptor subtype include cardioprotection,^[6,7] cancer,^[8–10] or glaucoma.^[11,12] Over the last two decades, many efforts have been made to search for potent and selective human A₃ antagonists, leading to a great variety of structurally diverse antagonist families.^[13–15]

In 2002, our research group described the tricyclic 1*H*,3*H*-pyrido[2,1-*f*]purine-2,4-dione family as a new xanthine class of highly potent A₃ antagonists,^[16] some of the most potent compounds are shown in Figure 1. Our previous SAR studies have shown three key points: 1) the substituent at position 3 has a mayor impact on the

potency against A₃ receptors, with propyl (as in compounds **1** and **2**) and cyclopropylmethyl (as in compound **3**) groups affording the most potent antagonistic effect, 2) the substituent at position 8 of the core structure afforded a certain degree of selectivity versus A₁ and A_{2A} receptors, and 3) the benzyl group at position 1 was required for activity and introduction of substituents on the benzyl group could also influence the selectivity against the different receptor subtypes.^[16]

The peculiarity of our structures, being xanthine-fused compounds, among A₃ receptor antagonists, led us to the present study with two major goals: first, to obtain a selective A₃ antagonist as our previous structures kept significant binding affinity for the A₁ receptor;^[16] and second, to study the binding mode of these compounds in a model of the hA₃ receptor.

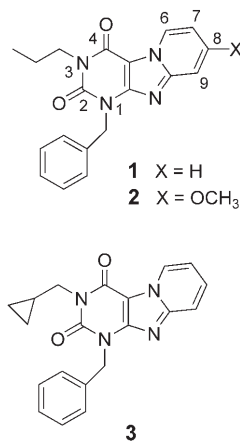


Figure 1. Representative hA₃ antagonists based on pyrido[2,1-*f*]purine-2,4-diones.

[a] Dr. S. Martín-Santamaría
Departamento de Química, Facultad de Farmacia
Universidad San Pablo CEU
Boadilla del Monte, Madrid (Spain)
Fax: (+34) 913510475
E-mail: smar.fcex@ceu.es

[b] Dr. E.-M. Priego, Dr. M.-J. Pérez-Pérez, Prof. M.-J. Camarasa
Instituto de Química Médica, C.S.I.C.
Juan de la Cierva 3, E-28006 Madrid (Spain)

[c] J. K. von Frijtag Drabbe Kuenzel, H. de Vries, Prof. A. P. IJzerman
Division of Medicinal Chemistry
Leiden/Amsterdam Center for Drug Research
P.O. Box 9502, 2300RA Leiden (The Netherlands)

Supporting information for this article is available on the WWW under <http://www.chemmedchem.org> or from the author.

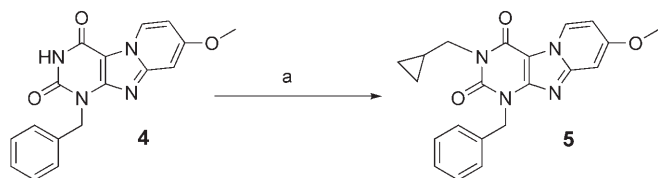
For our first goal, and based on our previous SAR data, we undertook the synthesis and biological evaluation of a new series of 1*H*,3*H*-pyrido[2,1-*f*]purine-2,4-diones that carry a methoxy group at position 8, a cyclopropylmethyl group at N3 and selected benzyl groups at position 1. The selection of the benzyl groups at position 1 was based on the Topliss batch-wise approach for the optimization of series where the lead compound has an unfused and unsubstituted benzene ring.^[17]

For our second goal, we performed molecular modeling studies of the newly synthesized A₃ antagonist **10** and a published hA₃ receptor model,^[18] using docking and molecular dynamic simulations techniques. It should be mentioned that molecular modeling of the A₃ receptor is being heavily investigated with at least three aims: to perform a pharmacophore analysis to obtain new lead compounds,^[19] to rationalize the increase in potency and/or selectivity of already synthesized compounds,^[20] or, as performed by Kim et al.,^[21] to get a better understanding of receptor activation. Our aim is clearly in the second category, using compound **10** as the ligand and the described model of the transmembrane domain of the hA₃ as the receptor.^[18] In the course of our studies, we found novel features of the previously described hA₃ model that can be of interest not only for our pyridopurinediones, but also for other A₃ antagonists.

Results and Discussion

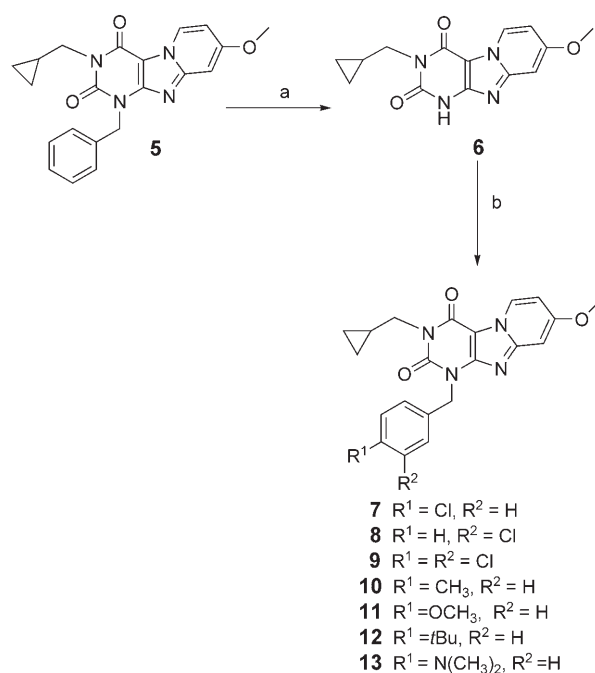
Chemistry

The synthesis of the core structure of 1*H*,3*H*-pyrido[2,1-*f*]purine-2,4-dione has been carried out according to our previously published procedure,^[16,22] and consisted of the treatment of 6-amino-1-benzyluracil with 2.5 equivalents of *N*-bromosuccinimide (NBS) to generate the intermediate 5,5-dibromo-6-imino derivative that reacted in situ with different substituted pyridines to afford the target tricyclic compounds.^[22] Based on this strategy, compound **4** was obtained from 6-amino-1-benzyluracil as previously described in 74% yield.^[16] Alkylation at position 3 with (bromomethyl)cyclopropane in the presence of DBU in acetonitrile at room temperature afforded compound **5** in 90% yield (Scheme 1).



Scheme 1. Reagents a) (bromomethyl)cyclopropane, DBU, CH₃CN, RT.

To introduce the selected benzyl groups at N1 according to the Topliss approach,^[17] the synthetic scheme undertaken involved the debenzilation of compound **5** to afford the NH-1 free compound, followed by the reaction with different benzyl halides (Scheme 2). Different debenzilation alternatives, using



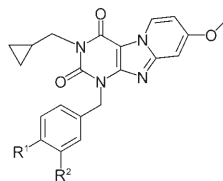
Scheme 2. Reagents a) HCO₂NH₄, Pd(OH)₂ (20%), EtOH, Δ, 5 h; b) ArX, DMF, K₂CO₃, RT, 1 h

similar described methods for 1,3-disubstituted uracils^[23] or xanthenes,^[24,25] did not lead us to the desired NH-free compound in a sufficient yield for our purposes. These difficulties to remove certain *N*-benzyl groups have already been described by other authors.^[24] In our hands, compound **6** was obtained in 42% yield by reaction of **5** with ammonium formate in the presence of Pd(OH)₂ in refluxing ethanol for 5 h, together with 54% of starting material.

Compound **6** was made to smoothly react with selected benzyl halides in DMF at room temperature and in the presence of K₂CO₃ as the base. The resulting structures (**7–12**) are shown in Scheme 2 and yields ranged from 81 to 93%. The synthesis of the 4-(dimethylamino)benzyl derivative **13** required the preparation of 4-(dimethylamino)benzyl chloride, which was synthesized according to described procedures,^[26] by reduction of 4-(dimethylamino)benzaldehyde to the corresponding alcohol, followed by transformation into the benzyl halide in the hydrochloride form. Reaction between compound **6** and this benzyl halide was carried out in the presence of K₂CO₃ and Et₃N to afford the desired N1-substituted compound **13** in 87% yield.

Binding Studies and Structure–Affinity Relationships

The synthesized compounds were tested in radioligand displacement assays to determine their affinities for the human adenosine A₁, A_{2A}, and A₃ receptors using [³H]DPCPX, [³H]ZM241385, and [¹²⁵I]AB-MECA, respectively, as the specific radioligands. Human A₁ and A_{2A} receptors were stably expressed in membranes of CHO cells whereas human A₃ receptors were stably expressed in HEK 293 cells. The results are shown in Table 1, which also includes the previously syn-

Table 1. Affinities of 3-cyclopropylmethyl-8-methoxy-1*H*,3*H*-pyrido[2,1-*f*]purine-2,4-diones at adenosine hA₁, hA_{2A}, and hA₃ receptors.


Compd.	R ¹	R ²	K _i [nM] or % displacement ^[a]		
			hA ₁	hA _{2A}	hA ₃
5	H	H	27 ± 11	134 ± 61	2.4 ± 0.5
6	–	–	N.D.	462 ± 134	593 ± 274
7	Cl	H	26.5 %	12.6 %	17 ± 5
8	H	Cl	17.4 %	13 %	71 ± 15
9	Cl	Cl	13 %	3 %	45 ± 6
10	CH ₃	H	24 %	0 %	2.2 ± 0.1
11	OCH ₃	H	39.8 %	0 %	6.4 ± 0.6
12	<i>t</i> Bu	H	17.5 %	12 %	208 ± 91
13	N(CH ₃) ₂	H	19.8 %	N.D.	11 ± 5
1			50 ± 17	119 ± 23	4.0 ± 0.3
2			179 ± 34	44 %	10 ± 1
3			40.9 %	242 ± 73	4.2 ± 1.1

[a] Percent displacement at [1 μM] (n = 2, average) or K_i ± SEM (nM, n = 3).

thesized compounds **1**, **2**, and **3**^[16] for comparative purposes. The new synthesized compounds **6–12** were also tested in a radioligand binding assay for the human adenosine A_{2B} receptor using [³H]MRS1754 as the radioligand. Little if any displacement of the radioligand (< 10%) was detected at 1 μM (data not shown), suggesting that the compounds are not active on human adenosine A_{2B} receptors.

Most of the synthesized compounds showed nanomolar affinities for the human adenosine A₃ receptor. For example, compound **5**, the prototype of this new series of 1*H*,3*H*-pyrido[2,1-*f*]purine-2,4-diones, had a K_i of 2.4 nM. However, this compound showed low selectivity versus the A₁ and A_{2A} receptors. As expected, substitutions at the benzyl moiety at N1 had a major impact on both the affinity and the selectivity against the different adenosine receptor subtypes. Thus, the 4-chlorobenzyl derivative **7** had a slightly reduced affinity for the hA₃ receptor compared to **5**, but more importantly, it lost its affinity for hA₁ and hA_{2A} receptors, so that selectivity was significantly increased. The 3-chlorobenzyl derivative (**8**) was also a selective A₃ antagonist, although its affinity was reduced compared to that of the 4-chlorobenzyl analogue (**7**). In accordance with these data, the 3,4-dichlorosubstituted benzyl derivative **9** showed a marked selectivity for the hA₃ receptor and an affinity that was intermediate between those of the mono-substituted compounds **7** and **8**. More pronouncedly, the 4-methylbenzyl derivative (**10**) combined a very high affinity for hA₃ (K_i = 2.2 nM) with lack of affinity for the A₁ and A_{2A} receptors, thereby becoming the most potent and selective A₃ antagonist among the 1*H*,3*H*-pyrido[2,1-*f*]purine-2,4-diones tested so far. The 4-methoxybenzyl derivative (**11**) afforded quite a similar profile both in activity and selectivity, as did the 4-(dimethylamino)benzyl derivative **13**. However, the affinity for the hA₃ receptor of the bulkier 4-*t*Bu-benzyl derivative (**12**) was re-

duced 90-fold compared to the 4-CH₃ benzyl derivative (**10**). These data point to the importance of the benzyl substituent at position N1 with regard to the potency and selectivity of this family of adenosine receptor antagonists versus the different receptor subtypes.

Molecular Modeling

With the aim of proposing a binding mode for this family of compounds and to rationalize the potency and selectivity of compound **10**, we were prompted to perform molecular modeling studies, including docking analysis and MD simulations, where experimental data could be integrated and rationalized. We first analyzed the hypothetical binding location of the 1*H*,3*H*-pyrido[2,1-*f*]purine-2,4-diones on the hA₃ receptor by undertaking a docking study for a few selected compounds from this family of A₃ antagonists. This study was followed by a MD simulation of the complex between the receptor and the most potent antagonist, compound **10**, to have a better understanding of the requirements for the binding of this particular family of antagonists.

In the absence of the 3D structure of the hA₃ receptor, models based on the structure of rhodopsin have been used as suitable templates for the resting state,^[27] which resembles an antagonist-like state. Thus, for the docking study, we employed the previously described model of the transmembrane domain of the hA₃ receptor (PDB code: 1OEA), that was refined by us, and the automated docking program AutoDock.^[28] The putative binding site of the ligands was located using CastP analysis,^[29] and included the residues that are known to be crucial for activity located in transmembrane (TM) segments 3, 5, 6, and 7,^[18] and the second extracellular loop (EL2). From visual inspection, the main interactions within the putative binding site agree with those proposed by Moro and co-workers for their triazoloquinoline^[30] and pyrazolotriazolopyrimidine derivatives.^[31] The ligands were placed inside the TM bundle, with the tricyclic ring system stacked between Phe 168 and the hydrogen-bonded Gln 167-Asn 250 pair, the condensed pyridine ring pointing toward EL2 (situated on top acting as a lid), and the CO group at position 4 oriented toward the NH group of Phe 168 (Figure 2). Interestingly, all the solutions provided by AutoDock for the different pyridopyrimidones inside the putative binding site of the hA₃ receptor shared this common orientation. Moreover, docking of some of our previously synthesized compounds^[16] possessing polar or more hindered side chains at N3, compounds that have very little affinity for the human A₃ receptor, did not lead to any solutions inside the putative binding site or they were not energetically favorable (data not shown). It is noticeable that the Gln 167-Asn 250 pair, as shown in Figure 2 has not been described before.

To validate and test the stability of the proposed binding mode, the **10**-hA₃ receptor complex was chosen to perform a MD simulation with positional restraints applied to Cα atoms. Also a MD simulation on the **3**-hA₃ receptor complex was carried out for comparison purposes, as compound **3** is the non-substituted analogue. Compound **10** remained docked along the simulations within the proposed binding pocket and re-

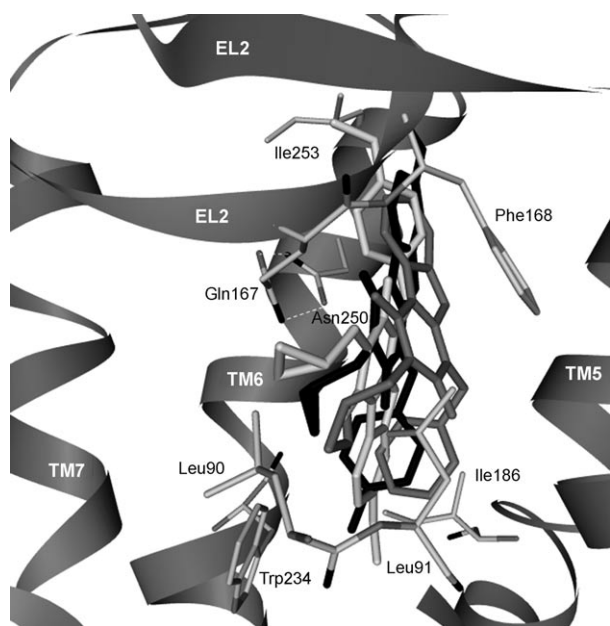


Figure 2. Superposition of some 1*H*,3*H*-pyrido[2,1-*f*]purine-2,4-diones derivatives considered in the docking positions obtained by AutoDock Ligands: black (compound **10**), light gray (compound **11**), and gray (compound **3**).

tained its starting conformation ($rsmd < 0.5 \text{ \AA}$ for all non-H atoms). Interestingly, while performing the MD simulation, the hydrogen-bonding pairing between Gln 167 (EL2) and Asn 250 (TM6) that probably stabilizes the folding of the EL2 hairpin over the TM bundles, was maintained during the whole length of the simulation. This prominent contact would not be possible in A_1 and A_2 receptors, as Gln at position 167 is unique to hA_3 receptors (this residue is a Glu in the A_1 receptor and a Leu in the A_{2A} and A_{2B} receptors) (Supporting Information, Figure S1). Thus, the hA_3 exclusive Gln-Asn pair, together with the highly conserved Phe 168, sterically delimits the cavity where compound **10** is confined within the putative binding site (Figure 3). The inspection of the van der Waals contributions of individual residues to the binding energy (Supporting Information, Figure S2A) reveals that major interactions arise from Gln 167 (EL2), Phe 168 (EL2), and Asn 250 (TM6). It has already been demonstrated that amino acids of the extracellular loop (EL2) could be involved in direct interactions with the ligands.^[32] In particular, there is an interaction between the CO group at position 4 of compound **10** and the NH group of the highly conserved Phe 168.

Looking for additional stabilizing interactions, it should be noted that the CO group at position 2 of **10** establishes a hydrogen bond with the hydroxyl group of Ser 181, coincident with strong electrostatic interaction energies (Supporting Information, Figure S2B). At the same time Ser 181 is hydrogen bonded to His 95. Both protonation states for His 95 were considered in our calculations. To allow this probable Ser 181-His 95 hydrogen bond, as already has been reported,^[33] the protonation on H_ϵ was chosen.

Hydrophobic ligand-receptor interactions were identified as important in the interaction of pyridipurinediones with the A_3

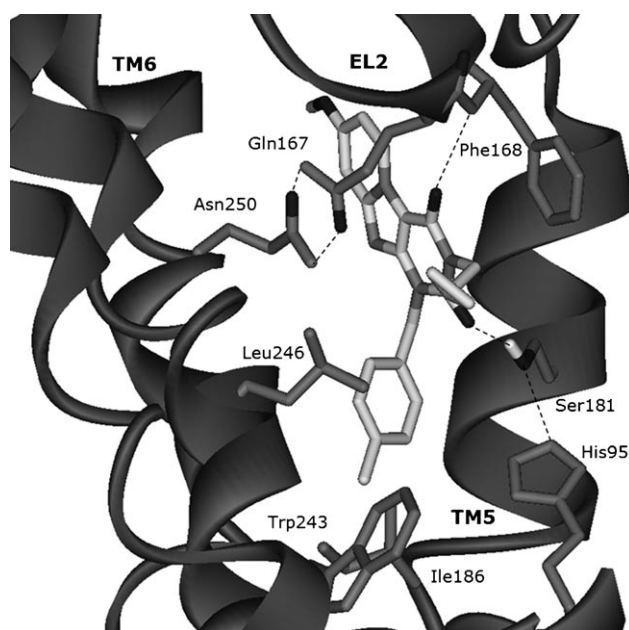


Figure 3. Proposed binding site for compound **10**, inserted in the cavity delimited by TM helices 3, 5, and 6, and EL2. Side chains of some amino acids important for ligand recognition are highlighted and labeled.

receptor. These are three regions occupied by substituents at positions 1, 3, and 8 of the core structure, which would be acting as three anchorage points inside the binding site. The first anchorage domain corresponds to position 8 of the condensed pyridine ring of the pyridopurine which is an important region in the SAR studies,^[16] and as described in this paper, the 8-OMe group is essential for A_3 selectivity. This group is located in a highly hydrophobic pocket in the hA_3 receptor made up by hA_3 exclusive residues such as Ile 253 (TM6, Thr in other subtypes of adenosine receptors), Tyr 254 (TM6, Leu or Phe in A_1 , A_{2A} , and A_{2B} adenosine receptors), Val 169-Ser 170-Val 171 backbone (EL2), and Met 172 (EL2, Ile, or Val in other subtypes). The presence of the 8-OMe group leads to van der Waals interaction energy values larger than those calculated for the complex with the unsubstituted compound **3** (data not shown).

The second and third anchorage points correspond to the cyclopropyl and benzyl chains at N3 and N1, respectively. The cyclopropyl chain at N3 of compound **10** is accommodated into the pocket delimited by the highly conserved residues Leu 90 (TM3), Leu 91 (TM3), Leu 246 (TM6), and Ile 268 (TM7), correlating with increased van der Waals interactions (Supporting Information, Figure S2A). The third hydrophobic pocket corresponds to the highly conserved region delimited by Ile 98 (TM3), Ile 186 (TM5), Trp 243 (TM6), and Leu 244 (TM6), which is occupied by the *p*-methylbenzyl substituent of **10** with favorable van der Waals interaction energies (Supporting Information, Figure S2A). It is interesting to note that the lack of the benzyl moiety at N1, as shown with compound **6**, results in a strong decrease in affinity for the A_3 receptor ($K_i = 593 \pm 274 \text{ nM}$). Similar results have been observed with our previous series of pyrido[2,1-*f*]purinediones.^[16] Selectivity for hA_3 was improved with substitution at the position 4 of the benzyl at

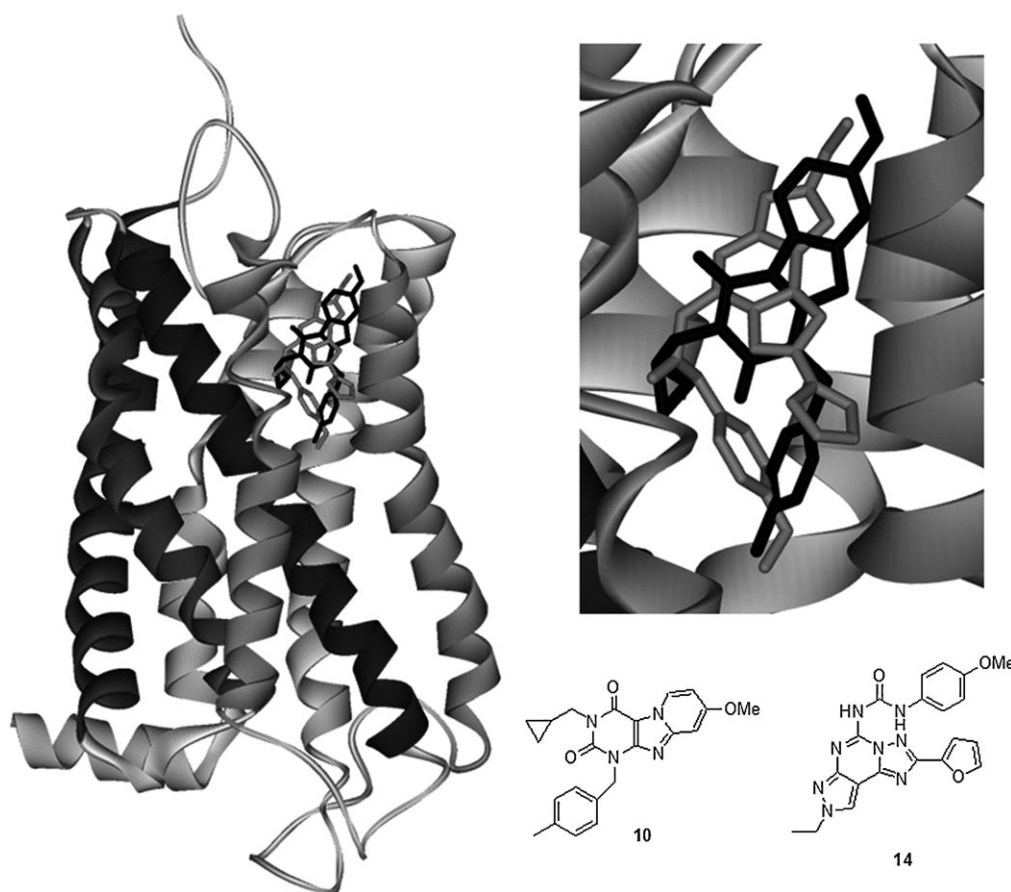


Figure 4. Superimposition of the docked structures of compounds **10** (black) and **14** (gray) inside the TM domain of hA₃ receptor. An enlarged detail is shown.

N1 by small substituents, methyl, or methoxy groups being the most selective. Substitution by a chloro atom, with lipophilicity similar to that of the methyl group but with different electronic properties, does not lead to such a high degree of selectivity. Derivatives with bulkier substituents such as 4-*tert*-butyl (**12**) do not fit appropriately in this well-defined region, leading to a decrease of affinity, which reveals that a steric control is taking place inside this cavity. Therefore, benzyl groups containing small electron donor substituents fill most efficiently this lipophilic pocket. Additionally, Trp243 has been shown to act as a switch in the TM6-mediated structural transition from the resting to the active state.^[34] Interactions with the benzyl group of compound **10** with this residue would not allow the reorientation of its side chain accompanying the inactive to active state transition. Thus, this benzyl group would be responsible for the improved potency in the antagonistic effect of this family of compounds, in agreement with favorable van der Waals interactions with Trp243.

The hA₃ exclusive Gln167-Asn250 pair, to the best of our knowledge has not been described before, and together with the highly conserved Phe168, could be one of the main characteristics defining the hA₃ subtype binding site. To establish if this novel feature applies exclusively to the binding mode of our pyridopyrimidones or also to other selective A₃ antagonists, docking studies were performed with the pyrazolotriazo-

lopyrimidine derivative **14**, a highly potent and selective A₃ antagonist ($K_i = 0.2$ nM).^[35] Superimposition of the docked structures of compounds **10** and **14** is shown in Figure 4. Interestingly, the binding mode of compound **14** makes use of binding regions common to those described above for our pyridopyrimidones: the tricyclic system of **14** is stacked between Phe168 and the Gln167-Asn250 pair, the methoxyphenyl group of **14** nicely occupies the region delimited by the Trp243 where the benzyl of compound **10** is lodged, the N6 atom forms a H-bond with the backbone NH of Phe168, analogously to the CO group at position 4 in compound **10**, and the furan O atom of **14** interacts with the hydroxyl group of Ser181, equivalent to the interaction with the CO at position 2 in compound **10**. An additional H-bond between the NH of the urea closer to the methoxybenzyl group, and the CO group of the Gln167 side chain was found.

Conclusions

By modifications performed at positions 1, 3, and 8 of our previously identified 1*H*,3*H*-pyrido[2,1-*f*]purine-2,4-diones, an increase in potency and, most remarkably, in selectivity against the human adenosine A₃ receptor has been achieved. The 3-cyclopropylmethyl-8-methoxy-1-(4-methylbenzyl)-1*H*,3*H*-pyrido[2,1-*f*]purine-2,4-dione (**10**) described herein, is a highly selec-

tive hA₃ antagonist with a K_i = 2.2 nM, and with no affinity for the A₁, A_{2A}, and A_{2B} receptors, being the most potent and selective A₃ antagonist among the 1*H*,3*H*-pyrido[2,1-*f*]purine-2,4-diones tested so far. Molecular modeling studies performed with several of our pyrido[2,1-*f*]purine-2,4-diones in the proposed model for the human A₃ receptor,^[18] resulted in the ligands being located in the putative binding site already proposed by other authors.^[30,31] The Gln 167-Asn 250 pair, maintained during the MD simulation, together with the highly conserved Phe 168, delimits the cavity where the pyrido[2,1-*f*]purine-2,4-diones are located, and could be an important feature related to the hA₃ subtype binding site. Van der Waals and electrostatic contributions of crucial residues to the binding of the pyridopurinediones are in good agreement with SAR data. Antagonist potency and selectivity are explained in terms of interactions with the key residue Trp 243, and other polar interactions involving Phe 168 and Ser 181. Similar interactions were found when the reported nonnucleoside A₃ selective antagonist **14** was subjected to docking studies inside the cavity. Therefore, and based on the studies described herein, our pyridopurinediones can be considered as an important tool that have provided further insights into the binding mode of ligands to the hA₃ receptor, contributing to this very active research area.

Experimental Section

Chemical Procedures

Melting points were obtained on a Reichert-Jung Kofler apparatus and are uncorrected. Microanalyses were obtained with a Heraeus CHN-O-RAPID instrument. Electrospray mass spectra were measured on a quadrupole mass spectrometer equipped with an electrospray source (Hewlett-Packard, LC/MS HP 1100). ¹H- and ¹³C NMR spectra were recorded on a Varian Gemini operating at 200 MHz (¹H) and 50 MHz (¹³C), respectively, on a Varian INNOVA 300 operating at 299 MHz (¹H) and 75 MHz (¹³C), respectively, and Varian INNOVA-400 operating at 399 MHz (¹H) and 99 MHz (¹³C), respectively. Monodimensional ¹H and ¹³C spectra were obtained using standard conditions. 2D inverse proton detected heteronuclear one-bond shift correlation spectra were obtained using the Pulsed Field Gradient HSQC pulse sequence. Data were collected in a 2048 × 512 matrix with a spectral width of 3460 Hz in the proton domain and 22500 Hz in the carbon domain, and processed in a 2048 × 1024 matrix. The experiment was optimized for one bond heteronuclear coupling constant of 150 Hz. 2D inverse proton detected heteronuclear long range shift correlation spectra were obtained using the Pulsed Field Gradient HMBC pulse sequence. The HMBC experiment was acquired in the same conditions that HSQC experiment and optimized for long range coupling constants of 7 Hz. Analytical TLC was performed on silica gel 60 F254 (Merck) precoated plates (0.2 mm). Spots were detected under UV light (254 nm). Separations on silica gel were performed by preparative centrifugal circular thin layer chromatography (CCTLC) on a ChromatotronR (Kiesegel 60 PF 254 gipshaltig (Merck)), layer thickness (1 or 2 mm), flow rate (4 or 8 mL min⁻¹, respectively). Flash column chromatography was performed with silica gel 60 (230–400 mesh) (Merck). All experiments involving water-sensitive compounds were conducted under scrupulously dry conditions. Acetonitrile was dried by refluxing over calcium hy-

dride. Anhydrous *N,N'*-dimethylformamide was purchased from Aldrich.

1-Benzyl-3-cyclopropylmethyl-8-methoxy-1*H*,3*H*-pyrido[2,1-*f*]purine-2,4-dione (5). (Bromomethyl)cyclopropane (226 μL, 2.33 mmol) and DBU (255 μL, 1.71 mmol) were added to a solution of **4**^[16] (500 mg, 1.55 mmol) in dry CH₂Cl₂ (15.5 mL). The mixture was stirred at room temperature for 6 h. Then, volatiles were removed and the residue was taken up in CH₂Cl₂ (150 mL) and washed with 1 N HCl (100 mL), water (100 mL), and brine (100 mL). The organic phase was dried (MgSO₄), filtered, and evaporated. The residue was purified by column chromatography using CH₂Cl₂:acetone (30:1) as eluent, to afford 506 mg (90%) of the title compound **5** as a white solid. Mp (CH₂Cl₂:MeOH): 198–200 °C. MS (ES, positive mode): *m/z* 377 [(*M*+1)⁺], 399 [(*M*+Na)⁺]. ¹H NMR (CDCl₃): δ = 0.47 (m, 4H, CH₂), 1.32 (m, 1H, CH), 3.95 (m, 5H, 3-NCH₂, OCH₃), 5.38 (s, 2H, 1-NCH₂), 6.75 (dd, *J* = 7.4, 2.6 Hz, 1H, H-7), 6.99 (d, *J* = 2.2 Hz, 1H, H-9), 7.26–7.58 (m, 5H, Ph), 8.84 ppm (d, *J* = 7.3 Hz, 1H, H-6). ¹³C NMR (CDCl₃): δ = 3.84 (CH₂), 10.19 (CH), 45.53 (3-NCH₂), 46.63 (1-NCH₂), 55.86 (OCH₃), 95.28 (C-9), 101.08 (C-4a), 107.59 (C-7), 127.74, 127.91, 128.50, 128.61, 136.52 (C-6, Ph), 149.97, 151.46, 151.70 (C-2, C-9a, C-10a), 154.79 (C-4), 161.51 ppm (C-8). Anal. (C₂₁H₂₀N₄O₃) C, H, N.

3-Cyclopropylmethyl-8-methoxy-1*H*,3*H*-pyrido[2,1-*f*]purine-2,4-dione (6). Pd(OH)₂ (20%) (350 mg) was added to a stirred solution of **5** (350 mg, 0.93 mmol) in EtOH (18 mL), and the mixture was heated to reach 80 °C. Then, ammonium formate was added (469 mg, 7.44 mmol), and the reaction mixture was heated at 80 °C for 1 h. Another portion of ammonium formate (469 mg, 7.44 mmol) was added and heating was continued for 5 h. Na₂SO₄·10H₂O was added and the mixture was allowed to reach room temperature, filtered, and the filtrate was evaporated. The residue was purified by flash column chromatography (florsyl) using CH₂Cl₂:MeOH (40:1) as eluent to afford 184 mg (54%) of **5** from the fastest moving fractions; the slowest moving fractions afforded 112 mg (42%) of the title compound **6** as a white solid. Mp (CH₂Cl₂:MeOH): 297–299 °C. MS (ES, positive mode): *m/z* 287 [(*M*+1)⁺], 313 [(*M*+Na)⁺]. ¹H NMR ([D₂O]DMSO): δ = 0.49 (m, 4H, CH₂), 1.29 (m, 1H, CH), 3.77 (d, *J* = 7.0 Hz, 2H, 3-NCH₂), 3.92 (s, 3H, OCH₃), 6.89 (dd, *J* = 7.3, 2.6 Hz, 1H, H-7), 7.11 (d, *J* = 2.2 Hz, 1H, H-9), 8.75 (d, *J* = 7.3 Hz, 1H, H-6), 11.99 ppm (br s, 1H, NH-1). ¹³C NMR (CDCl₃): δ = 3.53 (CH₂), 10.15 (CH), 43.72 (3-NCH₂), 56.15 (OCH₃), 95.40 (C-9), 99.94 (C-4a), 107.30 (C-7), 127.55 (C-6), 149.85, 150.55, 151.28 (C-2, C-9a, C-10a), 154.58 (C-4), 161.08 ppm (C-8). Anal. (C₁₄H₁₄N₄O₃) C, H, N.

General Procedure for the preparation of *N'*-substituted-3-cyclopropylmethyl-8-methoxy-1*H*,3*H*-pyrido[2,1-*f*]purine-2,4-diones.

K₂CO₃ (2.6 equiv) was added to a stirred solution of **6** (1 equiv) in anhydrous DMF (2 mL) and the mixture was stirred at RT for 1 h. Then, the corresponding benzyl halide (1.2 equiv) was added, and the reaction mixture was heated at 40 °C for 3 h. After cooling to RT, volatiles were removed, and the residue was taken up in EtOAc (20 mL) and washed with a saturated NaHCO₃ solution (20 mL). The organic phase was dried (Na₂SO₄), filtered, and evaporated. The residue was purified by CCTLC on the Chromatotron using hexane:EtOAc (2:1) as eluent.

1-(4-Chlorobenzyl)-3-cyclopropylmethyl-8-methoxy-1*H*,3*H*-pyrido[2,1-*f*]purine-2,4-dione (7). Following the general procedure, reaction of **6** (44 mg, 0.15 mmol) with K₂CO₃ (28 mg, 0.20 mmol) and 4-chlorobenzylbromide (36 mg, 0.18 mmol) yielded 51 mg (81%) of the title compound **7** as a white solid. Mp (CH₂Cl₂:MeOH): 218–220 °C. MS (ES, positive mode): *m/z* 411 [(*M*+1)⁺], showing the Cl isotopic pattern. ¹H NMR (CDCl₃): δ = 0.47 (m, 4H, CH₂), 1.31 (m, 1H, CH), 3.94 (m, 5H, 3-NCH₂, OCH₃), 5.33 (s, 2H, 1-NCH₂), 6.76 (dd, *J* = 7.2, 2.6 Hz, 1H, H-7), 6.98 (d, *J* = 2.4 Hz,

1H, H-9), 7.28 (d, $J=8.3$ Hz, 2H, Ph), 7.51 (d, $J=8.3$ Hz, 2H, Ph), 8.84 ppm (d, $J=7.3$ Hz, 1H, H-6). ¹³C NMR (CDCl₃): $\delta=3.84$ (CH₂), 10.18 (CH), 45.57, 45.97 (3-NCH₂, 1-NCH₂), 55.89 (OCH₃), 95.28 (C-9), 107.69 (C-7), 127.94, 128.67, 130.19, 133.67, 135.02 (C-6, Ph), 149.97, 151.25, 151.66 (C-2, C-9a, C-10a), 154.70 (C-4), 161.61 ppm (C-8). Anal. (C₂₂H₁₉ClN₄O₃) C, H, N.

1-(3-Chlorobenzyl)-3-cyclopropylmethyl-8-methoxy-1H,3H-pyrido[2,1-f]purine-2,4-dione (8). Following the general procedure, reaction of **6** (31 mg, 0.11 mmol) with K₂CO₃ (20 mg, 0.14 mmol) and 3-chlorobenzyl bromide (16 μ L, 0.12 mmol) yielded 43 mg (97%) of the title compound **8** as a white solid. Mp (CH₂Cl₂:MeOH): 225–226 °C. MS (ES, positive mode): m/z 411 [(M+1)⁺], showing the Cl isotopic pattern. ¹H NMR (CDCl₃): $\delta=0.45$ (m, 4H, CH₂), 1.30 (m, 1H, CH), 3.92 (m, 5H, 3-NCH₂, OCH₃), 5.32 (s, 2H, 1-NCH₂), 6.74 (dd, $J=7.3$, 2.4 Hz, 1H, H-7), 6.96 (d, $J=2.4$ Hz, 1H, H-9), 7.27 (dd, $J=3.8$, 1.3 Hz, 2H, Ph), 7.42 (td, $J=4.3$, 1.5 Hz, 1H, Ph), 7.51 (s, 1H, Ph), 8.82 ppm (d, $J=7.3$ Hz, 1H, H-6). ¹³C NMR (CDCl₃): $\delta=3.81$ (CH₂), 10.15 (CH), 45.54, 46.02 (3-NCH₂, 1-NCH₂), 55.85 (OCH₃), 95.27 (C-9), 101.02 (C-4a), 107.68 (C-7), 126.74, 127.87, 127.93, 128.53, 129.74, 134.27, 138.41 (C-6, Ph), 149.93, 151.18, 151.60 (C-2, C-9a, C-10a), 154.63 (C-4), 161.55 ppm (C-8). Anal. (C₂₁H₁₉ClN₄O₃) C, H, N.

3-Cyclopropylmethyl-1-(3,4-dichlorobenzyl)-8-methoxy-1H,3H-pyrido[2,1-f]purine-2,4-dione (9). Following the general procedure, reaction of **6** (42 mg, 0.15 mmol) with K₂CO₃ (26 mg, 0.19 mmol) and 3,4-dichlorobenzyl bromide (41 mg, 0.17 mmol) yielded 59 mg (90%) of the title compound **9** as a white solid. Mp (CH₂Cl₂:MeOH): 214–216 °C. MS (ES, positive mode): m/z 445 [(M+1)⁺], showing the isotopic 2Cl pattern. ¹H NMR (CDCl₃): $\delta=0.47$ (m, 4H, CH₂), 1.30 (m, 1H, CH), 3.94 (m, 5H, 3-NCH₂, OCH₃), 5.30 (s, 2H, 1-NCH₂), 6.75 (dd, $J=7.3$, 2.6 Hz, 1H, H-7), 6.97 (d, $J=2.4$ Hz, 1H, H-9), 7.39 (m, 2H, Ph), 7.65 (s, 2H, Ph), 8.82 ppm (d, $J=7.3$ Hz, 1H, H-6). Anal. ¹³C NMR (CDCl₃): $\delta=3.83$ (CH₂), 10.16 (CH), 45.52, 45.58 (3-NCH₂, 1-NCH₂), 55.88 (OCH₃), 95.31 (C-9), 101.05 (C-4a), 107.75 (C-7), 127.92, 128.16, 130.43, 130.63, 131.91, 132.50, 136.68 (C-6, Ph), 149.97, 151.05, 151.60 (C-2, C-9a, C-10a), 154.58 (C-4), 161.64 ppm (C-8). Anal. (C₂₁H₁₈Cl₂N₄O₃) C, H, N.

3-Cyclopropylmethyl-8-methoxy-1-(4-methylbenzyl)-1H,3H-pyrido[2,1-f]purine-2,4-dione (10). Following the general procedure, reaction of **6** (35 mg, 0.12 mmol) with K₂CO₃ (22 mg, 0.16 mmol) and 4-methylbenzyl bromide (26 mg, 0.14 mmol) yielded 42 mg (90%) of the title compound **10** as a white solid. Mp (CH₂Cl₂:MeOH): 189–191 °C. MS (ES, positive mode): m/z 391 [(M+1)⁺]. ¹H NMR (CDCl₃): $\delta=0.46$ (m, 4H, CH₂), 1.31 (m, 1H, CH), 2.31 (s, 3H, CH₃), 3.94 (m, 5H, 3-NCH₂, OCH₃), 5.34 (s, 2H, 1-NCH₂), 6.73 (dd, $J=7.2$, 2.4 Hz, 1H, H-7), 6.99 (d, $J=2.4$ Hz, 1H, H-9), 7.12 (d, $J=7.8$ Hz, 2H, Ph), 7.46 (d, $J=7.8$ Hz, 2H, Ph), 8.83 ppm (d, $J=7.5$ Hz, 1H, H-6). ¹³C NMR (CDCl₃): $\delta=3.83$ (CH₂), 10.17 (CH), 21.13 (CH₃), 45.49, 46.37 (3-NCH₂, 1-NCH₂), 55.83 (OCH₃), 95.25 (C-9), 101.07 (C-4a), 107.51 (C-7), 127.86, 128.68, 129.14, 133.54, 137.44 (C-6, Ph), 149.93, 151.42, 151.67 (C-9a, C-2, C-10a), 154.76 (C-4), 161.45 ppm (C-8). Anal. (C₂₂H₂₂N₄O₃) C, H, N.

3-Cyclopropylmethyl-8-methoxy-1-(4-methoxybenzyl)-1H,3H-pyrido[2,1-f]purine-2,4-dione (11). Following the general procedure, reaction of **6** (43 mg, 0.15 mmol) with K₂CO₃ (27 mg, 0.20 mmol) and 4-methoxybenzyl chloride (23 μ L, 0.17 mmol) yielded 57 mg (93%) of the title compound **11** as a white solid. Mp (CH₂Cl₂:MeOH): 195–197 °C. MS (ES, positive mode): m/z 407 [(M+1)⁺], 429 [(M+Na)⁺]. ¹H NMR (CDCl₃): $\delta=0.47$ (m, 4H, CH₂), 1.29 (m, 1H, CH), 3.76 (s, 3H, OCH₃), 3.93 (m, 5H, 3-NCH₂, OCH₃), 5.30 (s, 2H, 1-NCH₂), 6.72 (dd, $J=7.4$, 2.5 Hz, 1H, H-7), 6.83 (d, $J=8.7$ Hz, 2H, Ph), 6.98 (d, $J=2.6$ Hz, 1H, H-9), 7.53 (d, $J=8.7$ Hz, 2H, Ph), 8.82 ppm (d, $J=7.3$ Hz, 1H, H-6). ¹³C NMR (CDCl₃): $\delta=3.82$ (CH₂), 10.16 (CH), 45.47, 46.08 (1-NCH₂, 3-NCH₂), 55.18 (Ph OCH₃),

55.83 (OCH₃), 95.22 (C-9), 101.09 (C-4a), 107.50 (C-7), 113.77, 128.76, 128.86, 130.29, 159.14 (C-6, Ph), 149.92, 151.38, 151.65 (C-2, C-9a, C-10a), 154.75 (C-4), 161.46 ppm (C-8). Anal. (C₂₂H₂₂N₄O₄) C, H, N

1-(4-Tert-butylbenzyl)-3-cyclopropylmethyl-8-methoxy-1H,3H-pyrido[2,1-f]purine-2,4-dione (12). Following the general procedure, reaction of **6** (31 mg, 0.11 mmol) with K₂CO₃ (20 mg, 0.14 mmol) and 4-tert-butylbenzyl bromide (20 μ L, 0.12 mmol) yielded 46 mg (97%) of the title compound **12** as a white solid. Mp (CH₂Cl₂:MeOH): 183–186 °C. MS (ES, positive mode): m/z 433 [(M+1)⁺]. ¹H NMR (CDCl₃): $\delta=0.46$ (m, 4H, CH₂), 1.30 [m, 10H, C-(CH₃)₃, CH], 3.93 (m, 5H, 3-NCH₂, OCH₃), 5.35 (s, 2H, 1-NCH₂), 6.73 (dd, $J=7.4$, 2.6 Hz, 1H, H-7), 6.98 (d, $J=2.4$ Hz, 1H, H-9), 7.34 (d, $J=8.3$ Hz, 2H, Ph), 7.51 (d, $J=8.6$ Hz, 1H, Ph), 8.82 ppm (d, $J=7.3$ Hz, 1H, H-6). ¹³C NMR (CDCl₃): $\delta=3.83$ (CH₂), 10.16 (CH), 31.25 [C(CH₃)₃], 35.45 [C(CH₃)₃], 45.48, 46.23 (3-NCH₂, 1-NCH₂), 55.81 (OCH₃), 95.22 (C-9), 101.05 (C-4a), 107.48 (C-7), 125.38, 127.83, 128.42, 133.48, 149.90, 150.55 (C-6, Ph, C-9a), 151.44, 151.68 (C-2, C-10a), 154.74 (C-4), 161.42 ppm (C-8). Anal. (C₂₅H₂₈N₄O₃) C, H, N.

3-Cyclopropylmethyl-1-(4-dimethylaminobenzyl)-8-methoxy-1H,3H-pyrido[2,1-f]purine-2,4-dione (13). Following the general procedure, reaction of **6** (55 mg, 0.19 mmol) with K₂CO₃ (35 mg, 0.25 mmol), 4-dimethylaminobenzyl chloride hydrochloride^[26] (52 mg, 0.25 mmol) and Et₃N (35 μ L, 0.25 mmol) yielded 76 mg (87%) of the title compound **13** as an amorphous solid. MS (ES, positive mode): m/z 420 [(M+1)⁺]. ¹H NMR (CDCl₃): $\delta=0.46$ (m, 4H, CH₂), 1.28 (m, 1H, CH), 2.91 [s, 6H, N(CH₃)₂], 3.94 (m, 5H, 3-NCH₂, OCH₃), 5.28 (s, 2H, 1-NCH₂), 6.67 (d, $J=8.5$ Hz, 2H, Ph), 6.72 (dd, $J=7.4$, 2.4 Hz, 1H, H-7), 6.99 (d, $J=2.4$ Hz, 1H, H-9), 7.52 (d, $J=8.8$ Hz, 2H, Ph), 8.82 ppm (d, $J=7.6$ Hz, 1H, H-6). ¹³C NMR (CDCl₃): $\delta=3.86$ (CH₂), 10.20 (CH), 40.62 [N(CH₃)₂], 45.48 (3-NCH₂), 46.24 (1-NCH₂), 55.85 (OCH₃), 95.25 (C-9), 107.43, 112.27, 127.87, 130.25 (C-6, C-7, Ph), 149.94, 151.71, 152.02 (C-9a, C-10a, C-2), 154.83 (C-4), 161.43 ppm (C-8). Anal. (C₂₃H₂₅N₅O₃) C, H, N.

Radioligand Binding Studies

Radioligand binding studies were performed on stably transfected cell lines expressing human adenosine receptors. CHO cells expressing the human adenosine A₁ receptor were obtained from Dr. A. Townsend-Nicholson. These cells were cultured at 37 °C in a 5% CO₂ atmosphere in a 1:1 mixture of DMEM/F12, 2 mM Glutamax (a stable analogue of glutamine), 10% newborn calf serum with 50 IU/mL penicillin, and 50 mg mL⁻¹ streptomycin. Dr. S. Rees kindly provided CHO cells expressing the human A_{2A} and A_{2B} receptor. These cells were cultured at 37 °C in a 5% CO₂ atmosphere in a 1:1 mixture of DMEM/F12, 2 mM Glutamax, 10% newborn calf serum, 1 mg mL⁻¹ G418 with 50 IU/mL penicillin, and 50 mg mL⁻¹ streptomycin. HEK 293 cells expressing human adenosine A₃ receptors were from Dr. K.-N. Klotz. These cells were cultured at 37 °C in a 7% CO₂ atmosphere in a mixture of DMEM, 2 mM Glutamax, 10% newborn calf serum, 0.5 mg mL⁻¹ G418 with 50 IU mL⁻¹ penicillin, and 50 mg mL⁻¹ streptomycin. Confluent cells expressing the human A₁, A_{2A}, and A_{2B} receptor or semiconfluent cells expressing the human A₃ adenosine receptor were trypsinized and centrifuged for 10 min at 1000 rpm. The cell pellets were resuspended in 50 mM Tris/HCl (pH 7.4) at room temperature and homogenized on ice for 5 s at position 8 with an Ystral homogenizer. The homogenate was centrifuged for 45 min at 12 700 rpm in an SW-30 rotor at 4 °C. The resulting pellet was resuspended in 50 mM Tris/HCl (pH 7.4) at room temperature. Adenosine deaminase, 2 IU mL⁻¹, was added, and aliquots were stored at -80 °C. Stock solutions of ligands were made in DMSO. The final concentration of DMSO in the assay did not exceed 1%. [³H]DPCPX and [¹²⁵I]AB-

MECA were obtained from Amersham, and [^3H]ZM241385 and [^3H]MRS1754 were obtained from Tocris Cookson, Ltd. (Northpoint, U.K.).

Adenosine A_1 Receptor. Membranes containing 40 μg of protein were incubated in a total volume of 400 μL of 50 mM Tris/HCl (pH 7.4) and [^3H]DPCPX (final concentration, 1.6 nM) for 1 h at 25 °C in a shaking water bath. Nonspecific binding was determined in the presence of 10 μM CPA. The incubation was terminated by filtration over Whatman GF/B filters under reduced pressure with a Brandell harvester. Filters were washed three times with ice cold buffer and placed in scintillation vials. Emulsifier Safe (3.5 mL) was added, and after 2 h, radioactivity was counted in an LKB rack β scintillation counter.

Adenosine A_{2A} Receptor. Membranes containing 40 μg of protein were incubated in a total volume of 400 μL of 50 mM Tris/HCl (pH 7.4) and [^3H]ZM241385 (final concentration, 2.0 nM) for 2 h at 25 °C in a shaking water bath. Nonspecific binding was determined in the presence of 100 μM CPA. The incubation was terminated by filtration over Whatman GF/B filters under reduced pressure with a Brandell harvester. Filters were washed four times with ice cold buffer and placed in scintillation vials. Emulsifier Safe (3.5 mL) was added, and after 2 h, radioactivity was counted in an LKB rack β scintillation counter.

Adenosine A_{2B} receptor. Membranes containing 11 μg of protein were incubated in a total volume of 100 μL of 50 mM Tris/HCl, 0.1% CHAPS, ADA 1U mL $^{-1}$ (pH 7.4) and [^3H]MRS1754 (final concentration, 1.2 nM) for 1 h at 25 °C in a shaking water bath. Nonspecific binding was determined in the presence of 1 μM NECA. The incubation was terminated by filtration over Whatman GF/C filters under reduced pressure with a Brandell harvester. Filters were washed three times with ice cold 50 mM Tris/HCl pH 7.4 and placed in vials. Radioactivity was counted by a β counter.

Adenosine A_3 Receptor. Membranes containing 20–40 μg of protein were incubated in a total volume of 100 μL of 50 mM Tris/HCl, 10 mM MgCl $_2$, 1 mM EDTA, 0.01% CHAPS (pH 7.4), and [^{125}I]AB-MECA (final concentration, 0.10 nM) for 1 h at 37 °C in a shaking water bath. Nonspecific binding was determined in the presence of 100 μM R-PIA. The incubation was terminated by filtration over Whatman GF/B filters under reduced pressure with a Brandell harvester. Filters were washed three times with ice cold buffer and placed in vials. Radioactivity was counted by a β counter.

Computational Methods

The geometry of compounds **3**, **5**, **6**, **7**, **9**, **10**, **11**, and **14** were first optimized using the ab initio quantum chemistry program Gaussian 98^[36] and the HF/3-21G* basis set. Partial atomic charges were then obtained using the RESP^[37] methodology with the 6-31G(d) basis set.

Different conformers of compounds **3**, **5**, **6**, **7**, **9**, **10**, **11**, **14**, as well as the previously described 1-benzyl-8-phenyl-1*H*,3*H*-pyrido-[2,1-*f*]purine-2,4-dione and 1-benzyl-3-[(*E*)-3-methoxycarbonyl-2-propenyl]-1*H*,3*H*-pyrido-[2,1-*f*]purine-2,4-dione^[16] (data not shown) were docked in different orientations using the genetic algorithm implemented in AutoDock,^[28] and the refined form of human adenosine A_3 receptor (see below) as the target protein, by randomly changing the torsion angles and overall orientation of the molecule. A volume for exploration was defined in the shape of a three-dimensional cubic grid (30 \times 30 \times 30 \AA^3) with a spacing of 0.375 \AA that enclosed the putative binding site, which was located using castP analysis,^[29] and included the residues that are known to be crucial for activity^[18] and EL2. At each grid point, the receptor's atomic affinity potentials for carbon, aromatic carbon, oxygen, ni-

trogen, and hydrogen atoms were precalculated for rapid intra- and intermolecular energy evaluation of the docking solutions for each inhibitor.

The 3D structure of the transmembrane domain of the human adenosine A_3 receptor as built using homology modeling from the X-ray structure of bovine rhodopsin^[27] was retrieved from the Protein Data Bank^[38] (access number 1OEA). It is generally accepted that this model is a suitable template for the resting state of the receptor, which resembles an antagonist-bound state. Molecular dynamic simulations were carried out using the SANDER module in AMBER 6.^[39] The updated (parm99) second generation^[40] AMBER force field was used. SHAKE^[41] was applied to all bonds, and the integration time step was 1 fs. A fixed dielectric constant of 4.0 was used for all calculations.

The structure of the adenosine A_3 receptor was minimized with backbone constraints (5 kcal mol $^{-1}$ \AA^{-2}) on the secondary structure (5000 steps). The compound **10**–receptor complex was energy minimized (4000 steps), heated (from 0 to 300 K in 10 ps), and equilibrated (from 10 to 200 ps). Distance restraints (10 kcal mol $^{-1}$ \AA^{-2}) were applied to maintain the hydrogen bonds (2.8 \pm 0.1 \AA) between the backbone NH of Phe168 and the carbonyl of compound **10**, as these electrostatic interactions were thought to be of prime importance for complex stabilization. This restraint was removed thereafter and the system coordinates were then collected every 5 picoseconds for 1800 ps, which yielded an ensemble of 180 structures for each complex for further analysis. The geometries obtained during the trajectory from 1600 to 2000 ps (a total of 20) were averaged and energy minimized. The C α atoms were kept fixed at the positions originally determined because of the absence of the lipid environment in the molecular dynamic simulations. Molecular mechanics interaction energies between different parts of the system were calculated using the ANAL module of AMBER, and electrostatics were computed with DelPhi, following the procedure described in detail elsewhere.^[42]

Acknowledgements

This work has been supported by grants of the Spanish MEC (SAF2003-07219-C02-01 and SAF2006-12713-C02). E-M. P. has a CSIC contract from the I3P programme financed by the Fondo Social Europeo (F.S.E.). S.M.-S. thanks the Spanish MEC for a Ramón y Cajal contract.

Keywords: A_3 antagonist • adenosine receptors • molecular modeling • pyridopurinediones • structure–activity relationships

- [1] B. B. Fredholm, A. P. IJzerman, K. A. Jacobson, K. N. Klotz, J. Linden, *Pharmacol. Rev.* **2001**, *53*, 527–552.
- [2] Q. Y. Zhou, C. Y. Li, M. E. Olah, R. A. Johnson, G. L. Stiles, O. Civelli, *Proc. Natl. Acad. Sci. USA* **1992**, *89*, 7432–7436.
- [3] M. P. Abbracchio, R. Brambilla, S. Ceruti, H. O. Kim, D. von Lubitz, K. A. Jacobson, F. Cattabeni, *Mol. Pharmacol.* **1995**, *48*, 1038–1045.
- [4] H. Ali, O. H. Choi, P. F. Fraundorfer, K. Yamada, H. M. S. Gonzaga, M. A. Beaven, *J. Pharmacol. Exp. Ther.* **1996**, *276*, 837–845.
- [5] E. A. van Schaick, K. A. Jacobson, H. O. Kim, A. P. IJzerman, M. Danhof, *Eur. J. Pharmacol.* **1996**, *308*, 311–314.
- [6] Z. G. Gao, J. B. Blaustein, A. S. Gross, N. Melman, K. A. Jacobson, *Biochem. Pharmacol.* **2003**, *65*, 1675–1684.
- [7] J. P. Headrick, J. Peart, *Vasc. Pharmacol.* **2005**, *42*, 271–279.
- [8] S. Merighi, P. Mirandola, K. Varani, S. Gessi, E. Leung, P. G. Baraldi, M. A. Tabrizi, P. A. Borea, *Pharmacol. Ther.* **2003**, *100*, 31–48.

- [9] S. Gessi, K. Varani, S. Merighi, E. Cattabriga, A. Avitabile, R. Gavioli, C. Fortini, E. Leung, S. Mac Lennan, P. A. Borea, *Mol. Pharmacol.* **2004**, *65*, 711–719.
- [10] L. Madi, A. Ochaion, L. Rath-Wolfson, S. Bar-Yehuda, A. Erlanger, G. Ohana, A. Harish, O. Merimski, F. Barer, P. Fishman, *Clin. Cancer Res.* **2004**, *10*, 4472–4479.
- [11] M. Y. Avila, R. A. Stone, M. M. Civan, *Invest. Ophthalmol. Visual Sci.* **2002**, *43*, 3021–3026.
- [12] T. Okamura, Y. Kurogi, K. Hashimoto, S. Sato, H. Nishikawa, K. Kiryu, Y. Nagao, *Bioorg. Med. Chem. Lett.* **2004**, *14*, 3775–3779.
- [13] S. Moro, Z. G. Gao, K. A. Jacobson, G. Spalluto, *Med. Res. Rev.* **2006**, *26*, 131–159.
- [14] P. G. Baraldi, M. A. Tabrizi, F. Fruttarolo, A. Bovero, B. Avitabile, D. Preti, R. Romagnoli, S. Merighi, S. Gessi, K. Varani, P. A. Borea, *Drug Dev. Res.* **2003**, *58*, 315–329.
- [15] C. E. Muller, *Curr. Top. Med. Chem.* **2003**, *3*, 445–462.
- [16] E. M. Priego, J. K. von Frijtag Drabbe Kuenzel, A. P. IJzerman, M. J. Camarasa, M. J. Pérez-Pérez, *J. Med. Chem.* **2002**, *45*, 3337–3344.
- [17] J. G. Topliss, *J. Med. Chem.* **1977**, *20*, 463–469.
- [18] Z. G. Gao, S. K. Kim, T. Biadatti, W. Z. Chen, K. Lee, D. Barak, S. G. Kim, C. R. Johnson, K. A. Jacobson, *J. Med. Chem.* **2002**, *45*, 4471–4484.
- [19] A. Tafi, C. Bernardini, M. Botta, F. Corelli, M. Andreini, A. Martinelli, G. Ortore, P. G. Baraldi, F. Fruttarolo, P. A. Borea, T. Tuccinardi, *J. Med. Chem.* **2006**, *49*, 4085–4097.
- [20] O. Lenzi, V. Colotta, D. Catarzi, F. Varano, G. Filacchioni, C. Martini, L. Trincavelli, O. Ciampi, K. Varani, F. Marighetti, E. Morizzo, S. Moro, *J. Med. Chem.* **2006**, *49*, 3916–3925.
- [21] S. K. Kim, Z. G. Gao, L. S. Jeong, K. A. Jacobson, *J. Mol. Graphics Modell.* **2006**, *25*, 562–577.
- [22] M. J. Pérez-Pérez, E. M. Priego, M. L. Jimeno, M. J. Camarasa, *Synlett* **2002**, 155–157.
- [23] M. Botta, V. Summa, R. Saladino, R. Nicoletti, *Synth. Commun.* **1991**, *21*, 2181–2187.
- [24] A. R. Beauglehole, S. P. Baker, P. J. Scammells, *J. Med. Chem.* **2000**, *43*, 4973–4980.
- [25] M. H. Holschbach, T. Fein, C. Krummeich, R. G. Lewis, W. Wutz, U. Schwabe, D. Unterlugauer, R. A. Olsson, *J. Med. Chem.* **1998**, *41*, 555–563.
- [26] G. B. Barlin, L. P. Davies, S. J. Ireland, M. M. L. Ngu, *Aust. J. Chem.* **1989**, *42*, 1133–1146.
- [27] K. Palczewski, T. Kumasaka, T. Hori, C. A. Behnke, H. Motoshima, B. A. Fox, I. Le Trong, D. C. Teller, T. Okada, R. E. Stenkamp, M. Yamamoto, M. Miyano, *Science* **2000**, *289*, 739–745.
- [28] G. M. Morris, D. S. Goodsell, R. S. Halliday, R. Huey, W. E. Hart, R. K. Belew, A. J. Olson, *J. Comput. Chem.* **1998**, *19*, 1639–1662.
- [29] J. Liang, H. Edelsbrunner, C. Woodward, *Protein Sci.* **1998**, *7*, 1884–1897.
- [30] V. Colotta, D. Catarzi, F. Varano, F. R. Calabri, O. Lenzi, G. Filacchioni, C. Martini, L. Trincavelli, F. Deflorian, S. Moro, *J. Med. Chem.* **2004**, *47*, 3580–3590.
- [31] S. Moro, P. Braiuca, F. Deflorian, C. Ferrari, G. Pastorin, B. Cacciari, P. G. Baraldi, K. Varani, P. A. Borea, G. Spalluto, *J. Med. Chem.* **2005**, *48*, 152–162.
- [32] M. E. Olah, K. A. Jacobson, G. L. Stiles, *J. Biol. Chem.* **1994**, *269*, 24692–24698.
- [33] S. Kehraus, S. Gorzalka, C. Hallmen, J. Iqbal, C. E. Muller, A. D. Wright, M. Wiese, G. M. König, *J. Med. Chem.* **2004**, *47*, 2243–2255.
- [34] C. Hallmen, M. Wiese, *J. Comput.-Aided Mol. Des.* **2006**, *20*, 673–684.
- [35] P. G. Baraldi, B. Cacciari, R. Romagnoli, G. Spalluto, K. N. Klotz, E. Leung, K. Varani, S. Gessi, S. Merighi, P. A. Borea, *J. Med. Chem.* **1999**, *42*, 4473–4478.
- [36] M. J. Frisch, G. W. Trucks, H. B. Schlegel, G. E. Scuseria, M. A. Robb, J. R. Cheeseman, V. G. Zakrzewski, J. A., Jr., Montgomery, R. E. Stratmann, J. C. Burant, S. Dapprich, J. M. Millam, A. D. Daniels, K. N. Kudin, M. C. Strain, O. Farkas, J. Tomasi, V. Barone, M. Cossi, R. Cammi, B. Mennucci, C. Pomelli, C. Adamo, S. Clifford, J. Ochterski, G. A. Petersson, P. Y. Ayala, Q. Cui, K. Morokuma, D. K. Malick, A. D. Rabuck, K. Raghavachari, J. B. Foresman, J. Cioslowski, J. V. Ortiz, B. B. Stefanov, G. Liu, A. Liashenko, P. Piskorz, I. Komaromi, R. Gomperts, R. L. Martin, D. J. Fox, T. Keith, M. A. Al-Laham, C. Y. Peng, A. Nanayakkara, C. Gonzalez, M. Challacombe, P. M. W. Gill, B. G. Johnson, W. Chen, M. W. Wong, J. L. Andres, M. Head-Gordon, E. S. Replogle, and J. A. Pople, **1998**, *Gaussian 98*, Gaussian, Inc., Pittsburgh, PA.
- [37] C. I. Bayly, P. Cieplak, W. D. Cornell, P. A. Kollman, *J. Phys. Chem.* **1993**, *97*, 10269–10280.
- [38] H. M. Berman, J. Westbrook, Z. Feng, G. Gilliland, T. N. Bhat, H. Weissig, I. N. Shindyalov, P. E. Bourne, *Nucleic Acids Res.* **2000**, *28*, 235–242.
- [39] D. A. Case, D. A. Pearlman, J. W. Caldwell, T. E. Cheatham, III, W. S. Ross, C. L. Simmerling, T. A. Darden, K. M. Merz, R. V. Stanton, A. L. Cheng, J. J. Vincent, M. Crowley, V. Tsui, R. J. Radmer, Y. Duan, J. Pitera, I. Massova, G. L. Seibel, U. C. Singh, P. K. Weiner, P. A. Kollman, AMBER, version 6; Department of Pharmaceutical Chemistry, University of California, San Francisco, **1999**.
- [40] W. D. Cornell, P. Cieplak, C. I. Bayly, I. R. Gould, K. M. Merz, D. M. Ferguson, D. C. Spellmeyer, T. Fox, J. W. Caldwell, P. A. Kollman, *J. Am. Chem. Soc.* **1995**, *117*, 5179–5197.
- [41] J. P. Ryckaert, G. Ciccotti, H. J. C. Berendsen, *J. Comput. Phys.* **1977**, *23*, 327–341.
- [42] C. Pérez, M. Pastor, A. R. Ortiz, F. Gago, *J. Med. Chem.* **1998**, *41*, 836–852.

Received: July 19, 2007

Revised: September 21, 2007

Published online on November 14, 2007